

# Low-overhead Magic State Circuits with Transversal CNOTs

Nicholas Fazio,<sup>1,\*</sup> Mark Webster,<sup>2,\*</sup> and Zhenyu Cai<sup>3,4</sup>

<sup>1</sup>*Centre for Engineered Quantum Systems, School of Physics,  
The University of Sydney, Sydney, New South Wales 2006, Australia.*

<sup>2</sup>*Department of Physics & Astronomy, University College London, London, WC1E 6BT, United Kingdom*

<sup>3</sup>*Department of Materials, University of Oxford, Parks Road, Oxford OX1 3PH, United Kingdom*

<sup>4</sup>*Quantum Motion, 9 Sterling Way, London N7 9HJ, United Kingdom*

(Dated: January 20, 2025)

With the successful demonstration of transversal CNOTs in many recent experiments, it is the right moment to examine its implications on one of the most critical parts of fault-tolerant computation – magic state preparation. Using an algorithm that can recompile and simplify a circuit of consecutive multi-qubit phase rotations, we manage to construct fault-tolerant circuits for  $|CCZ\rangle$ ,  $|CS\rangle$  and  $|T\rangle$  states with minimal  $T$ -depth and also much lower CNOT depths and qubit counts than before. These circuits can play crucial roles in fault-tolerant computation with transversal CNOTs, and we hope that the algorithms and methods developed in this paper can be used to further simplify other protocols in similar contexts.

## I. INTRODUCTION

For quantum computers to realize their full potential, they must achieve fault tolerance at large scales, and the associated overheads need to be kept low to ensure reasonable device sizes and compute time. There have been several recent experimental demonstrations of quantum error correction (QEC) across a variety of architectures [1–4], substantiating that QEC does work in practice. The capabilities and limitations of these architectures are quite different, meaning that their respective approaches to large-scale fault tolerance will differ as they utilize schemes that take advantage of the strengths of their architecture.

One critical component of fault tolerance is the generation of high-quality non-Clifford resources, the so-called magic states, which have been the subject of concerted research. The resources required for preparing and distilling magic states have been massively reduced through a series of schemes [5–8], with recent work suggesting that the generation of  $|T\rangle$  states can have lower overheads than lattice-surgery logical CNOTs [8] for a certain range of target error rates.

In many cases the non-Clifford resources generated, namely  $|T\rangle$  states, must be further synthesized into other non-Clifford gates like CCZ to be implemented in a circuit. Addressing this need has been met with a series of approaches in both gate synthesis and state distillation. An early example is Jones’ fault-tolerant construction for implementing CCZ from eight  $T$  gates using techniques in synthesis [9, 10]. Later the connections between the phase polynomials of synthesis [11] and the triorthogonal matrices of magic state distillation [12] were identified, and unified under the portmanteau of synthillation [13], which combines the state distillation and gate

synthesis steps to further suppress error rates. Jones’ fault-tolerant construction was then recognized as an example of a synthillation scheme with code parameters  $[[8,3,2]]$ . Re-expressing extant gadgets has also been used to derive magic measurements for making schemes more accessible [5], or catalyzed state factories for reducing overheads [14].

When considering explicit implementation and optimisation of schemes for magic state distillation and the closely related synthillation, most of the prior works focus on 2D qubit connectivity using lattice surgery. On the other hand, significant experimental progress has been made in multiple hardware platforms such as trapped ions and neutral atoms [1–3, 15] in demonstrating additional qubit connectivity and transversal CNOT gates available between code patches. These capabilities have significant potential to reduce the spacetime overhead of fault-tolerant computation [16] and naturally, significant room for improvements to magic state preparation circuits in this context.

In this work, considering the availability of transversal CNOTs and the enhanced connectivity between logical qubits, we have devised an algorithm for optimising CNOT+ $T$  magic state preparation circuits, achieving low qubit counts, low CNOT depth and minimal  $T$  depth. The algorithm leverages SWAP gates to reduce the CNOT counts, absorbing SWAPs into the state initialization round. For architectures where arbitrary SWAP gates are cheap, this compilation strategy can be extended to more general settings. The algorithm adopts a greedy approach which can be adapted for different requirements, for example, optimising for CNOT count rather than CNOT depth. Our work is complementary to recent results in magic state preparation [8] since all our circuits start with states prepared in  $|T\rangle$ , which inherently lends itself to better schemes for high-quality magic states. Moreover, the required output error rates for the schemes preparing  $|T\rangle$  do not need to be high because synthillation further improves the error rates for the final non-Clifford gate.

\* These authors contributed equally to this work. Corresponding authors [nicholas.fazio@sydney.edu.au](mailto:nicholas.fazio@sydney.edu.au), [mark.webster@ucl.ac.uk](mailto:mark.webster@ucl.ac.uk), [cai.zhenyu.physics@gmail.com](mailto:cai.zhenyu.physics@gmail.com).

We start this paper by introducing the fault-tolerant CCZ scheme of Jones [9] in Sec. II as a motivating example, describing its components and the ways that this scheme can be reformulated. In Sec. III we introduce the concept of phase rotation operators and outline our algorithm for simplifying blocks of CNOTs. At the end of the section and also in Sec. IV, we apply our algorithm to construct low overhead fault-tolerant schemes for CCZ, CS and  $T$  as shown in Figs. 5, 7 and 8. This is followed by a brief resource analysis of our CCZ circuit in Sec. V and further discussion in Sec. VI.

## II. MOTIVATING EXAMPLE: FAULT-TOLERANT CCZ

Selinger [11] proposed a way to implement  $CC(iZ)$  (which is equivalent to  $CS \cdot CCZ$ ) using a circuit of only  $T$ -depth one as shown in Fig. 1. Single  $Z$  errors on any  $T$  and  $T^\dagger$  gates in this circuit will propagate to qubit 3. Hence, Jones [9] proposed encoding qubit 3 into a phase-flip repetition code depicted in Fig. 2, which can detect single  $Z$  errors on any  $T$  and  $T^\dagger$ , suppressing the failure rate of the CCZ from  $p$  to  $p^2$ . This circuit can then be used for preparing the CCZ resource state  $|CCZ\rangle$  by inputting  $|+\rangle$  on the first three qubits. For the rest of the paper, we will often use  $T$  gates to refer to both  $T$  and  $T^\dagger$ , which should be obvious from the context.

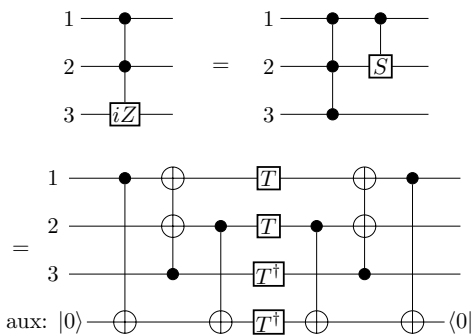


FIG. 1. Circuit for implementing  $CC(iZ)$ .

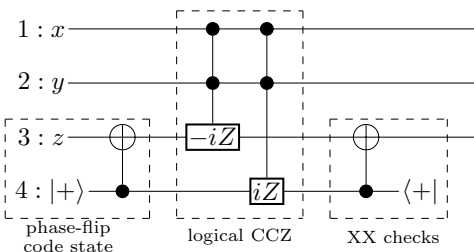


FIG. 2. Circuit for fault-tolerant CCZ. The CCZs here can be implemented using Fig. 1 and its conjugate, thus there are two additional auxiliary qubits used that are not shown here.

The explicit circuit constructed by Jones for  $|CCZ\rangle$  preparation is shown in Fig. 3, with additional auxiliary

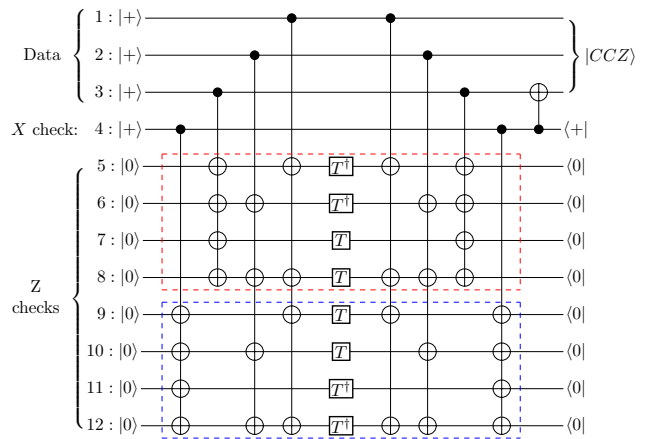


FIG. 3. Circuit for distilling CCZ states from  $T/T^\dagger$  gates. The red and blue dashed boxes denote the  $T$  gates that are used for implementing a particular  $CC(iZ)$  gate.

qubits performing  $Z$  checks on the  $T$  gates, detecting  $X$  errors. These auxiliary qubits can also be used to facilitate lattice surgery [14]. Let us focus on only the  $T$  gate error suppression power of the circuit, ignoring the memory error and Clifford gate errors and considering only the error of the  $T$  gates. In this case, no  $X$  error will occur for  $T$  gates implemented using gate teleportation, and thus the  $Z$  checks will act trivially and will not contribute to the error suppression. Hence, to reduce the qubit overhead of the circuit while keeping the same  $T$  gate error suppression power, these  $Z$ -check auxiliary qubits can be removed by permuting all the  $T$  gates through the CNOTs, resulting in a series of multi-qubit phase rotations as shown in Fig. 4 [17]. Here multi-qubit phase rotations (or  $Z$ -parity rotations) are simply unitaries generated by tensor products of  $Z$ , which is rigorously defined later in Sec. III. In this form, the raw action of  $T$  gates on the input states can be understood without worrying about the specific placement of  $T$  gates or Clifford gates. However, all of the  $T$  gates have now become multi-qubit  $\pi/8$  rotations that cannot be parallelised, leading to maximum  $T$ -depth. In the next section, we will discuss how to reduce the  $T$ -depth without introducing auxiliary qubits, maintaining the small qubit count of the circuit.

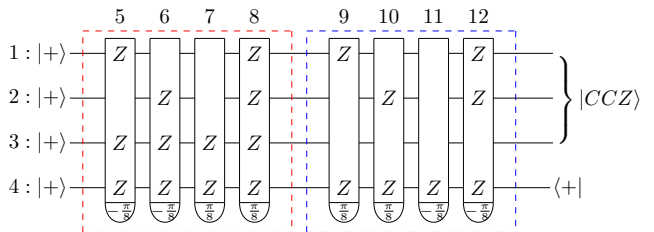


FIG. 4. Circuit for distilling CCZ states using multi-qubit  $\pi/8$  phase rotations. The index over each phase rotation denotes which  $T$  gate qubit it corresponds to in Fig. 3.

### III. ALGORITHMS FOR PHASE ROTATION PARALLELISATION

Similar to the fault-tolerant CCZ circuit in the last section, more general magic state distillation circuits can also be mapped into a series of phase rotation operators. In this section, we will detail the algorithm for converting a series of phase rotation operators to circuits composed of a qubit permutation followed by alternating blocks of the following two types:

- A series of CNOT gates; and
- Application of (possibly different) powers of T in parallel on each of the qubits.

The result of the algorithm is a circuit which has minimum T-depth without introducing auxiliary qubits, as well as low 2-qubit gate count and depth for the CNOT circuit blocks.

Our method is similar to the one set out in [10] to reduce T-depth, but introduces a new algorithm for synthesizing CNOT Clifford operators. This method expresses the Clifford operator as a circuit that consists of a qubit permutation followed by a series of two-qubit CNOT gates. After CNOT synthesis, we commute the permutation for each block through to the beginning of the circuit. The qubit permutation and initial CNOT block can typically be absorbed into the state preparation part of the circuit.

The structure of this section is as follows. We first introduce a notation for phase rotation operators and CNOT circuit blocks. We then show how to parallelize a set of independent phase rotation operators by conjugating a series of  $T$  operators by a CNOT Clifford operator. We then introduce our CNOT synthesis algorithm and finish with an example that illustrates the construction of a circuit for CCZ synthillation.

#### A. Notation for Phase Rotation and CNOT Operators

The **phase rotation operator** is defined as:

$$Z_{\mathbf{u}}^{\theta} := \exp(i\theta(I - Z(\mathbf{u}))) \propto \exp[-i\theta Z(\mathbf{u})]. \quad (1)$$

where  $\theta \in \mathbb{R}$  is an angle of rotation,  $\mathbf{u}$  is a binary vector of length  $n$  and  $Z(\mathbf{u}) := \prod_{0 \leq i < n} Z_i^{\mathbf{u}[i]}$  is the tensor product of  $Z$  operators that acts non-trivially on the qubits where  $\mathbf{u}[i] = 1$ . The phase rotation operator  $Z_{\mathbf{u}}^{\theta}$  has the following action on basis elements  $|\mathbf{e}\rangle$ :

$$Z_{\mathbf{u}}^{\theta} |\mathbf{e}\rangle = e^{i2\theta(\mathbf{u} \cdot \mathbf{e} \pmod{2})} |\mathbf{e}\rangle. \quad (2)$$

We consider a series of phase rotation operators  $\prod_{0 \leq i < m} Z_{\mathbf{u}_i}^{\theta_i}$  to be **independent** if the associated binary matrix  $U$  with columns  $\mathbf{u}_i$  is full-rank, i.e. the set of vectors  $\{\mathbf{u}_i\}_{0 \leq i < n}$  are linearly independent. We will also

use  $Z_i^{\theta}$  to denote a single-qubit rotation that acts non-trivially on qubit  $i$ .

We can express any CNOT circuit block as a Clifford operator  $CX(U)$  where  $U$  is an invertible binary matrix referred to as a **parity matrix** (see [18]). The operator  $CX(U)$  has symplectic matrix form  $\begin{bmatrix} U & 0 \\ 0 & (U^T)^{-1} \end{bmatrix}$  and has the following action on the computational basis element  $|\mathbf{e}\rangle$ :

$$CX(U) |\mathbf{e}\rangle = |U\mathbf{e}\rangle. \quad (3)$$

#### B. Parallelisation of Phase Rotation Operators

A set of independent phase rotations is equivalent to a series of  $T$  operators conjugated by a CNOT Clifford operator as set out in the following result:

**Theorem 1** (parallelisation of independent phase rotation operators). *Let  $\prod_{0 \leq i < n} Z_{\mathbf{u}_i}^{\theta_i}$  be a series of independent phase rotation operators on  $n$  qubits and let  $U$  be the invertible binary matrix with columns  $\mathbf{u}_i$ . The product of the phase rotation operators can be written as:*

$$\prod_{0 \leq i < n} Z_{\mathbf{u}_i}^{\theta_i} = CX(U)^{-1} \left( \prod_{0 \leq i < n} Z_i^{\theta_i} \right) CX(U).$$

**Proof:** For the computational basis element  $|\mathbf{e}\rangle$ ,  $CX(U) |\mathbf{e}\rangle = |U\mathbf{e}\rangle$  (see Equation (3)). Bit  $i$  of  $U\mathbf{e}$  is given by  $\mathbf{u}_i \cdot \mathbf{e}$  and so  $Z_i^{\theta_i}$  applies a phase of  $e^{i2\theta_i} \iff \mathbf{u}_i \cdot \mathbf{e} = 1 \pmod{2}$ . This is the same phase applied by the phase rotation operator  $Z_{\mathbf{u}_i}^{\theta_i}$  to  $|\mathbf{e}\rangle$  (see Equation (2)).

Applying the same logic to all  $0 \leq i < n$ , we have:

$$\prod_{0 \leq i < n} Z_i^{\theta_i} |U\mathbf{e}\rangle = \prod_{0 \leq i < n} e^{i2\theta_i(\mathbf{u}_i \cdot \mathbf{e} \pmod{2})} |U\mathbf{e}\rangle.$$

Noting that  $CX(U)^{-1} |U\mathbf{e}\rangle = |\mathbf{e}\rangle$ , the result follows.

#### C. Partition of Phase Rotations into Independent Sets

We have shown how to express a product of  $n$  independent phase rotation operators as a CNOT Clifford operator conjugating a parallel application of  $T$  operators on the qubits. In general, we have more than  $n$  phase rotation operators to simplify. In this case, we separate the phase rotations into a series of independent sets of rotations which correspond to a series of invertible binary matrices  $U_i$ , then apply the above result to each  $U_i$ . In [10], a polynomial-time algorithm is presented for finding independent sets of phase rotations using partitions of matroids. For our optimisation, we sample from all possible orderings of the phase rotations. We separate each ordering into sets of size  $n$ . We reject those which do not form independent sets, then simplify the CNOT circuit blocks as much as possible to find an optimal solution.

#### D. Simplification of CNOT Circuit Blocks

In this section, we describe an algorithm for simplifying a CNOT Clifford operator of the form  $CX(U)$  for some invertible binary matrix  $U$ . There may be many ways of expressing the operator as a circuit. Our objective is to express the operator in terms of an initial qubit permutation, followed by as few 2-qubit CNOT gates as possible.

Our method is a greedy algorithm which looks at all possible  $CNOT_{ij}$  operations at each step, selecting the one which results in a matrix with the lowest possible column and row-sums. The justification for this heuristic is as follows. For the operator  $CX(U)$ , effecting  $CNOT_{ij}$  is equivalent to replacing column  $j$  of  $U$  with the sum of columns  $i$  and  $j \bmod 2$  and this is similar to operations used in Gaussian elimination. When applying Gaussian elimination to a full-rank matrix, the end result is the identity. In this algorithm, we instead perform column operations so that the end result is a permutation matrix in which the sum of every row and every column is one. The algorithm selects the  $CNOT_{ij}$  at each step which gets us as close as possible to this end configuration. A detailed description is set out in Algorithm 1.

---

#### Algorithm 1 CNOT Synthesis

---

**Input:**

An invertible  $n \times n$  binary matrix  $U$ .

**Output:**

A permutation matrix  $P$  plus a series of row operations opList which generate  $U$  when applied to  $P$ .

**Method:**

#  $P$  will be modified by the algorithm and be returned as the permutation matrix

Set  $P := \text{transpose}(U)$

# list of  $CNOT_{ij}$  as ordered pairs  $(i,j)$

Set opList := []

# if  $P$  is a permutation matrix then  $\text{sum}(P) == n$

done := ( $\text{sum}(P) == n$ )

**while** not done **do**

# col and row-sums of matrix after applying  $CNOT_{ij}$   
 $w_{ij} = []$

**for**  $i$  in range( $n$ ) **do**

**for**  $j$  in range( $n$ ) **do**

**if**  $i \neq j$  **then**

$B := \text{copy}(P)$

$B[j] := B[i] + B[j]$

$w := \text{sorted}(\text{colSums}(B) + \text{rowSums}(B))$

$w_{ij}.\text{append}((w,i,j))$

**end if**

**end for**

**end for**

# choose  $(i,j)$  with min col and row sums after  $CNOT_{ij}$   
 $w_{i,j} = \min(w_{ij})$

# update  $P$  and opList

$P[j] := P[i] + P[j]$

opList.append( $(i,j)$ )

# Check if  $P$  is a permutation matrix

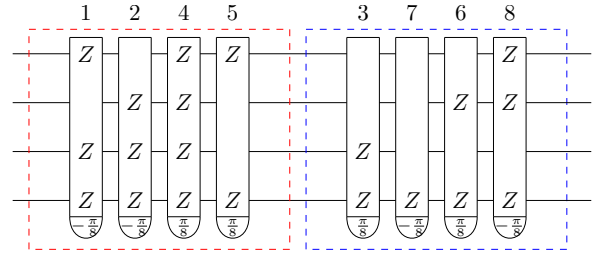
done := ( $\text{sum}(P) == n$ )

**end while**

return  $P$ , reversed(opList)

#### E. Fault-tolerant CCZ Example

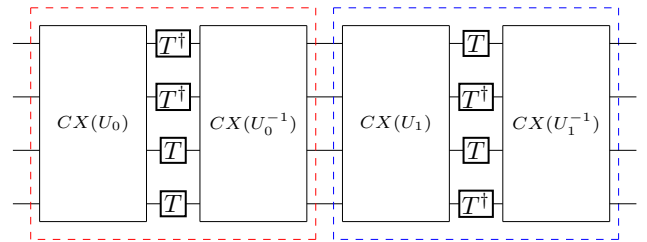
Let us now look back to the question of turning the series of phase rotations in the CCZ synthillation circuit of Fig. 4 into a circuit with maximally parallelized  $T$  without auxiliary qubits. There are 8 phase rotations acting on 4 qubits, hence, in order to parallelise them we need to first divide them into linearly independent sets as discussed in Sec. III C. By sampling all possible permutations, we find the following reordering of the phase rotation operators of Fig. 4:



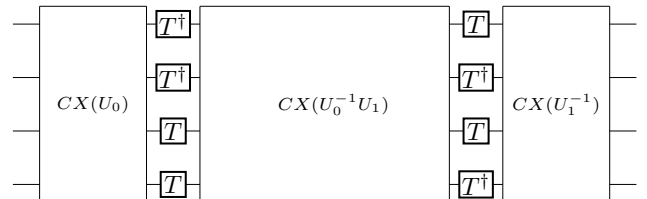
We partition the phase rotations into two blocks corresponding to the following invertible binary matrices:

$$U_0 := \begin{bmatrix} 1 & 0 & 1 & 1 \\ 0 & 1 & 1 & 0 \\ 1 & 1 & 1 & 0 \\ 1 & 1 & 1 & 1 \end{bmatrix}; \quad U_1 := \begin{bmatrix} 0 & 0 & 0 & 1 \\ 0 & 0 & 1 & 1 \\ 1 & 0 & 0 & 0 \\ 1 & 1 & 1 & 1 \end{bmatrix}.$$

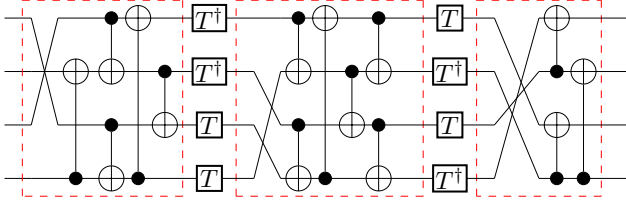
Using Theorem 1, we can write the phase rotations as CNOT Clifford operators conjugating parallel applications of  $T$  and  $T^\dagger$  operators:



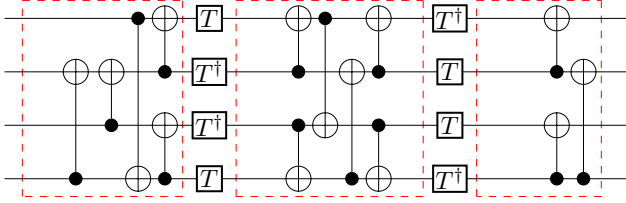
To simplify the CNOT blocks, we first group together adjacent blocks as follows:



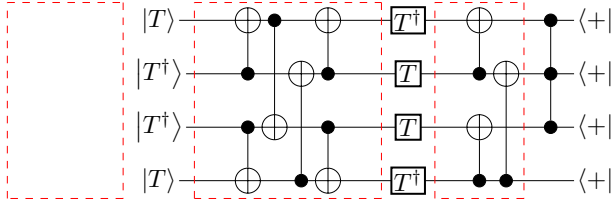
Applying Algorithm 1, we synthesize each CNOT block into a qubit permutation followed by a series of CNOT gates:



We commute all qubit permutations through to the beginning of the circuit by updating the CNOT gates and reordering the  $T/T^\dagger$  operators. In this case, the permutations cancel but this is not always the case. We obtain the following:



Absorbing the initial CNOT block and any residual qubit permutations into state preparation using the methods of Appendix A, and adding the final gates we derive the following circuit for fault-tolerant CCZ:



Using  $X|T\rangle = |T^\dagger\rangle$  and  $XT^\dagger X = T$ , we can further rewrite the circuit above purely in terms of  $T$ , CNOTs and  $X$  as shown in Fig. 5.

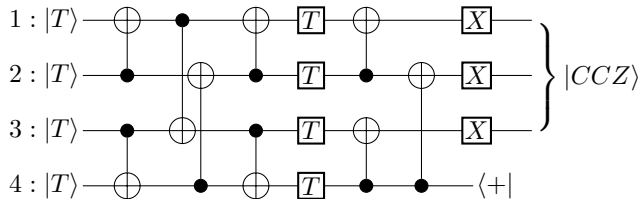


FIG. 5. Circuit for fault-tolerant CCZ. Note that the first layer of CNOTs only has depth 3. The CNOT gates in the circuit can be implemented using 2D nearest-neighbour connectivity.

## IV. MORE MAGIC STATE CIRCUITS

### A. Fault-tolerant CS gate

Let us now apply our CNOT synthesis algorithm from Sec. III to a new example with similar structure: a fault-tolerant CS gate.

In Sec. II we discussed the decomposition  $CC(iZ) = CS \cdot CCZ$  and how this was used by Jones [9] to construct a CCZ gate where any single  $T$  gate fault is detectable. In a similar way we derive a circuit that implements a CS gate that can tolerate single  $T$  gate faults shown in Fig. 6. This circuit may be understood as the fault-tolerant CCZ circuit of Fig. 2 with an additional  $CC(iZ)$  applied. Since the action on the third qubit is the identity it can be used to detect errors from the extra  $CC(iZ)$ , making the overall scheme fault-tolerant.

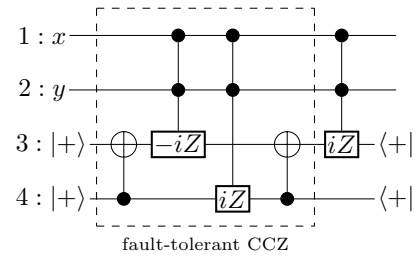
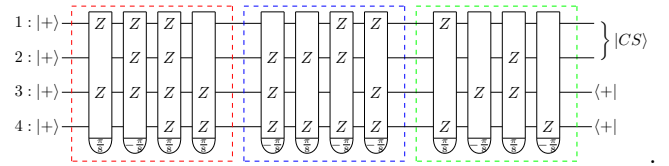


FIG. 6. Circuit for fault-tolerantly implementing a CS with faulty  $T$  gates. The  $CC(iZ)$ s here are implemented using Fig. 1 and its conjugate.

Following Sec. II, we may express the circuit of Fig. 6 in terms of 12 parallel  $T/T^\dagger$ , and then further convert that circuit into phase rotations. After regrouping the resultant phase rotations into independent sets we arrive at the following circuit<sup>1</sup>



We then apply the algorithm of Sec. III, and the sequence of phase rotations is transformed into alternating layers of CNOT circuits and transversal  $T/T^\dagger$ . SWAP gates and the initial CNOTs are then absorbed into the initial  $|+\rangle$  states so that the first  $T/T^\dagger$  layer can be incorporated as part of state initialization. We arrive at the fault-tolerant CS circuit of Fig. 7 where each CNOT layer has depth 1 or 2.

<sup>1</sup> This sequence of 12 phase rotations corresponds to the  $[[12,2,2]]$  code of Webster et al. [19], where transversal  $T$  implements a logical CS gate, or the  $NCS$  synthillation protocol of Campbell and Howard for  $N = 1$  [13].

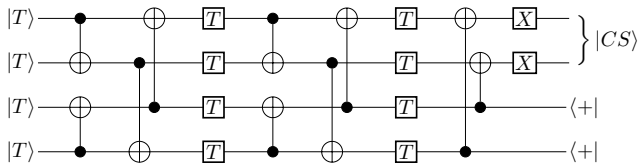
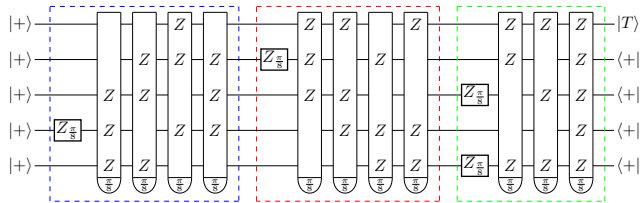


FIG. 7. Circuit for distilling CS states rearranged to use in-place parallel  $T/T^\dagger$  gates.

### B. T gate distillation circuit

Another application example is the well-studied 15-to-1  $T$  state distillation scheme derived from the  $[[15,1,3]]$  Reed-Muller code [20], which can be implemented using 24 logical patches with lattice surgery as depicted in Ref. [21]. As in previous sections, we can turn the circuit into a series of phase rotation operators as outlined by Litinski [17], and these rotations can be grouped into linearly independent sets as shown below.



Once again following the steps outlined in Sec. III, each group here can be implemented using parallel  $T$  gates and towers of CNOTs. With further simplifications, we can obtain Fig. 8.

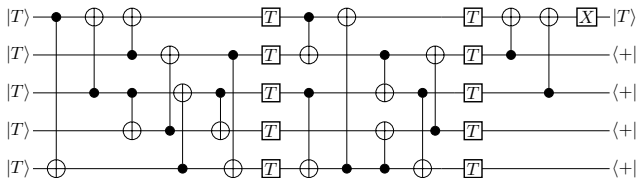


FIG. 8. Our simplified circuit for distilling T states. Its CNOT depth is  $5 + 4 + 2 = 11$ , and it can be implemented using nearest-neighbour connectivity.

## V. RESOURCE ANALYSIS

In this section we single out our construction for  $|CCZ\rangle$  synthillation and explore a low-space implementation for that scheme to demonstrate how these circuits may be used in practice.

The design of the circuit in figure 5 is intended to be favourable for architectures where transversal CNOTs can be implemented with low overhead. The majority of the circuit is comprised of parallel logical CNOTs. In addition, assuming transversal CNOTs are available then the  $T$  gates can also be done via injection, using a single

parallel CNOT cycle and adaptive  $S$  feedback. Overall the scheme takes 6 transversal CNOT rounds and 1 round set aside for the adaptive application of logical  $S$  gates.

This construction has a relatively low space cost since costs associated with transportation and auxiliary patches, which are utilised in lattice surgery, are eliminated when transversal CNOTs can be performed between arbitrary logical qubits. Furthermore, since 3 of the 4 data qubits are output qubits, there is limited scope for further space savings. On the other hand, space savings could be made as part of the schemes for  $T$  state preparation and injection. However, our goal here is not to prove rigorous overheads, so we make the simple assumption that the space cost for each logical qubit is identical because they all need to be initialised in  $|T\rangle$ . As an estimate let's assume that  $3d^2$  qubits are necessary per logical qubit:  $d^2$  for the code qubits, and another  $2d^2$  for any auxiliary and flag qubits. These qubit numbers will explicitly depend on the code and state preparation scheme used, but these numbers are an overestimate for existing schemes [6–8]. Thus the space cost is  $24d^2$  in total. When the  $S$  gate is not a native transversal logical of the code, extra space may be required to accommodate logical  $|S\rangle$  states via catalytic  $S$  gate teleportation [22]. The decoding time for the adaptive  $S$  correction is ultimately a key limitation for the time cost, but assuming that it can be done in 1 code cycle, then for a total of 7 code cycles a rough estimate for the spacetime cost is  $\sim 7 \times 24d^2 = 168d^2$ .

This spacetime cost is only for the CCZ synthillation stage and excludes the cost associated with preparing 8  $|T\rangle$  states. There are various magic state preparation schemes that could be used [6–8], with their own respective costs and output error rates.

After approximating the spacetime overhead of our circuit, let us next consider its error performance. To keep our analysis independent of particular decoders and preparation schemes we assume two distinct types of noise: a logical failure rate  $p_L$  on each logical qubit at each code cycle, and a  $|T\rangle$  preparation error rate

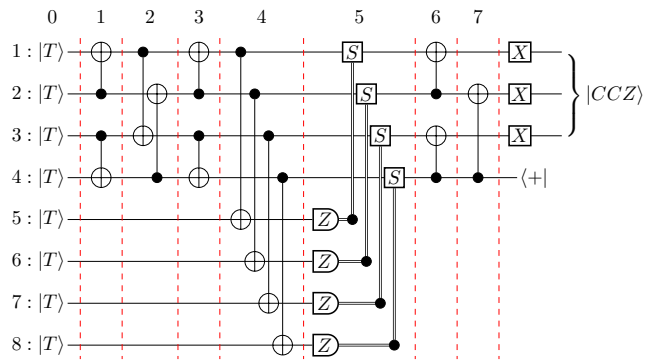


FIG. 9. Implementation of a fault-tolerant CCZ with explicit  $T$ -gadgets. Each round can be implemented using transversal CNOTs, with the exception of round 5. The amount of time necessary for round 5 is dependent on decoding time.

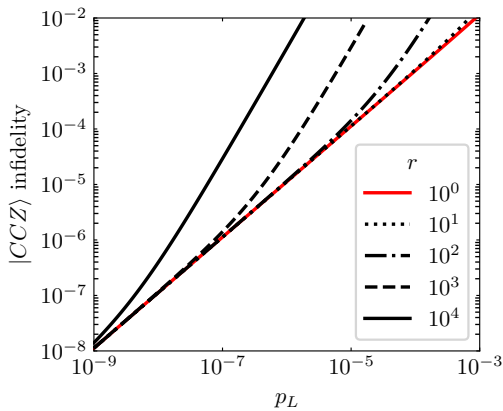


FIG. 10. State infidelity of an output  $|CCZ\rangle$  state using Fig. 9. In round 0  $|T\rangle$  states are implemented with  $Z$  errors at rate  $p_T = rp_L$ . Thereafter, at the end of each round each qubit experiences logical depolarising noise, including auxiliary qubits, at rate  $p_L$ .

$p_T = rp_L$  that is  $r$  times larger than the logical error rate. The scheme performance is shown in Fig. 10, using a depolarising noise model with rate  $p_L$  and a  $Z$  error only model at rate  $p_T$  on initialized states. We consider  $Z$  errors only for initialized  $|T\rangle$  because Pauli noise on the  $T$  state can effectively be viewed as phase errors, as discussed in Appendix B. Other noise models were considered, but the effect of noise bias [23] on both sources had a negligible impact on the performance and so the simplest model has been shown. This is mainly because many logical failures on the output qubits remain as logical failures regardless of which error occurred, accumulating in the final error of the state.

As expected, the performance is lower bounded by the logical error rate of the data qubits. These first order terms, together with second order terms in  $p_T$ , are the lowest order contributions to the  $|CCZ\rangle$  error rate around  $11.25p_L + 28p_T^2$ . Since the lowest order term with a  $p_T$  factor is  $28p_T^2$ , for the  $T$  gate's contribution to noise to be at the same order of magnitude as the target error rate of the preparation scheme,  $p_T$  should be around  $\sim 0.7\sqrt{p_L}$ . This means that the spacetime costs associated with  $|T\rangle$  preparation should only be as high as necessary to get below that target, which has a relatively small coefficient because of low CNOT depth.

Since we assume  $T$  states are all prepared at the beginning of the scheme, the  $T$  states that are for injection are idle until the parallel  $T$  round, as shown in Fig. 9. However, the inclusion of these idling errors has a negligible effect on the output rates because idling errors correspond to phase errors at each  $T$  location, which are all caught at first order. We typically have  $p_L^2 \ll p_T^2$ , meaning that these idling errors have a far smaller impact than errors from  $|T\rangle$  preparation. A far more significant factor to consider is the logical noise that can build up while decoding the injection measurement.  $Z$  errors

from such a source are unremarkable for the same reason as idling errors, however  $X$  and  $Y$  errors that are introduced during this time are typically going to contribute to the final error rate. Taking into account an arbitrary decoding time  $t_{\text{decode}}$ , the lowest order effects are  $(10.25 + t_{\text{decode}})p_L + 28p_T^2$ . Thus if the decoder is slow, the contribution to noise is notable.

Better and faster decoders are naturally of importance here. If the adaptive  $S$  gate has to be significantly delayed for decoding, then logical errors on the data qubits will accumulate. This scheme benefits codes with a transversal  $S$  and CNOT rather well, such as the color codes, but the decoders for color codes are not as performant as those for surface code which affects the achievable  $p_L$  for code distance  $d$ . The poor performance of color code decoders meant they were avoided for magic state cultivation [8], even though color codes would otherwise be a more natural fit for the later stages.

## VI. DISCUSSION

In this paper, by exploiting the transversal CNOT available in many hardware platforms, we are able to construct fault-tolerant circuits for generating distilled  $|CCZ\rangle$ ,  $|CS\rangle$  and  $|T\rangle$  states with very low spacetime overhead (Figs. 5, 7 and 8). This is done through an algorithm that compiles a series of  $\pi/8$ -phase rotations into a circuit with low CNOT depth and minimal  $T$ -depth, assuming free SWAPs given by the symmetry of the circuit or added connectivity of the hardware. This algorithm can be easily generalised to arbitrary phase rotations and also rotations in other bases, thus can be useful for compiling circuits in other contexts beyond magic state preparation. It will also be interesting to generalise this algorithm to rotations of mixed basis.

The  $CCZ$  circuit we obtain requires a workspace of at most 8 logical qubits and a minimum time overhead of 7 code cycles. On the other hand, circuits of the same  $T$  error suppression power carried out using lattice surgery with planar connectivity will require 18 logical qubits and  $8.5d$  code cycles [14], which is a factor of  $\sim 3d$  larger in the spacetime overhead. This shows that the additional connectivity enabling transversal CNOTs can indeed greatly reduce the spacetime overhead for magic state circuits. Note that this does not require full 3D connectivity, but only requires a thin slice of 3D structure with shallow height since the number of code patches needed in our circuits is small. The architecture to implement such a quasi-3D connectivity in 2D hardware using only local shuttling has been proposed in [24]. Besides being able to achieve the same  $T$  error suppression power as its lattice surgery counterpart, our circuit will also accumulate fewer code cycle errors due to the much shorter time required.

As mentioned in the last section, our circuits can be a key stage in magic state factories, but a previous stage is needed to prepare the incoming  $T$  states [6–8]. It will

also be interesting to consider whether the availability of transversal CNOTs, along with the methods used in this paper, can be used to further optimise  $T$  state preparation schemes.

## ACKNOWLEDGEMENTS

The authors would like to thank Craig Gidney for the valuable discussions. NF thanks his advisors Robin Harper and Stephen Bartlett for supporting this work and acknowledges support from the Australian Research Council via the Centre of Excellence in Engineered Quantum Systems (EQUS) project number CE170100009, and by the ARO under Grant Number: W911NF-21-1-0007. ZC acknowledges support from the EPSRC QCS Hub EP/T001062/1, EPSRC projects Robust and Reliable Quantum Computing (RoARQ, EP/W032635/1), Software Enabling Early Quantum Advantage (SEEQA, EP/Y004655/1) and the Junior Research Fellowship from St John's College, Oxford. MW acknowledges support from the EPSRC [grant numbers EP/S005021/1, EP/W032635/1].

## Appendix A: Circuit Compilation Tricks

Here is a list of circuit compilation tricks used to manipulate the circuits of the main text.

*a. Off-loading Z Rotations*  $Z$  rotations (including  $T$  gates) can be implemented in an out-of-place manner.

$$\text{---} \boxed{Z_\theta} \text{---} = \begin{array}{c} \bullet \\ \text{---} \\ \oplus \\ \text{---} \\ \bullet \end{array} \text{---} \boxed{Z_\theta} \text{---} \begin{array}{c} \bullet \\ \text{---} \\ \oplus \\ \text{---} \\ \bullet \end{array} \langle 0|$$

*b. Error propagation of CCZ* CCZ is a gate symmetric under the permutation of all three qubits. An  $X$  error on any one of the qubit will propagate to CZ on the other two qubits.

$$\begin{array}{c} \boxed{X} \\ \text{---} \\ \bullet \\ \text{---} \\ \bullet \\ \text{---} \\ \bullet \end{array} \text{---} \begin{array}{c} \bullet \\ \text{---} \\ \bullet \\ \text{---} \\ \bullet \end{array} \boxed{X} \text{---}$$

*c. Commuting CNOTs* An example of commuting one CNOT through another is shown here.

$$\begin{array}{c} \oplus \\ \text{---} \\ \bullet \\ \text{---} \\ \bullet \\ \text{---} \\ \oplus \end{array} \text{---} \begin{array}{c} \bullet \\ \text{---} \\ \bullet \\ \text{---} \\ \oplus \end{array} \text{---} = \begin{array}{c} \bullet \\ \text{---} \\ \oplus \\ \text{---} \\ \bullet \\ \text{---} \\ \oplus \end{array} \text{---} \begin{array}{c} \oplus \\ \text{---} \\ \bullet \\ \text{---} \\ \oplus \end{array} \text{---}$$

We are essentially commuting  $X$  in one of the CNOTs through the other CNOT to become  $X \otimes X$  with both  $X$ s controlled on the same qubit as the original CNOT before being permuted through.

When commuting a CNOT through another CNOT that acts on the same qubits but in reverse direction, the CNOT becomes a SWAP.

$$\begin{array}{c} \oplus \\ \text{---} \\ \bullet \\ \text{---} \\ \oplus \end{array} \text{---} \begin{array}{c} \bullet \\ \text{---} \\ \oplus \\ \text{---} \\ \bullet \end{array} \text{---} = \begin{array}{c} \times \\ \text{---} \\ \times \\ \text{---} \\ \times \end{array} \text{---} \begin{array}{c} \oplus \\ \text{---} \\ \bullet \\ \text{---} \\ \oplus \end{array} \text{---} = \begin{array}{c} \bullet \\ \text{---} \\ \oplus \\ \text{---} \\ \bullet \end{array} \text{---} \begin{array}{c} \times \\ \text{---} \\ \times \\ \text{---} \\ \times \end{array} \text{---}$$

*d. CNOT on  $|+\rangle$*  CNOTs act trivially on tensor products of  $|+\rangle$  since  $X$  gate acts trivially on  $|+\rangle$ .

*e. CNOT and CCZ* As we try to commute CNOT through CCZ, when the control qubit is in  $|0\rangle$ , nothing will happen, while when the control qubit is in  $|1\rangle$ , the  $X$  in the CNOT will propagate through the CZ in CCZ and become  $X \otimes Z$ . Correspondingly, it means that the CNOT will become a CNOT and a CZ when permute through CCZ. We can further permute CZ back through the CCZ while adding an  $X$  gate and using rule (b) above.

$$\begin{array}{c} \bullet \\ \text{---} \\ \bullet \\ \text{---} \\ \bullet \end{array} \text{---} \begin{array}{c} \bullet \\ \text{---} \\ \oplus \\ \text{---} \\ \bullet \end{array} \text{---} = \begin{array}{c} \bullet \\ \text{---} \\ \oplus \\ \text{---} \\ \bullet \end{array} \text{---} \begin{array}{c} \bullet \\ \text{---} \\ \bullet \\ \text{---} \\ \bullet \end{array} \text{---} \begin{array}{c} \bullet \\ \text{---} \\ \bullet \\ \text{---} \\ \bullet \end{array} \text{---} = \begin{array}{c} \bullet \\ \text{---} \\ \oplus \\ \text{---} \\ \bullet \end{array} \text{---} \boxed{X} \text{---} \begin{array}{c} \bullet \\ \text{---} \\ \bullet \\ \text{---} \\ \bullet \end{array} \text{---} \boxed{X} \text{---}$$

Similarly, when a CNOT acts on a CCZ state we have:

$$\begin{array}{c} \text{CCZ state} \\ \boxed{|+\rangle} \\ \bullet \\ \text{---} \\ \bullet \\ \text{---} \\ \bullet \end{array} \text{---} \begin{array}{c} \bullet \\ \text{---} \\ \oplus \\ \text{---} \\ \bullet \end{array} \text{---} = \begin{array}{c} \text{CCZ state} \\ \boxed{|+\rangle} \\ \bullet \\ \text{---} \\ \bullet \\ \text{---} \\ \bullet \end{array} \text{---} \begin{array}{c} \bullet \\ \text{---} \\ \bullet \\ \text{---} \\ \bullet \end{array} \text{---} \boxed{X} \text{---}$$

*f. Transforming between  $T$  and  $T^\dagger$*   $T$  and  $T^\dagger$  can be transformed into one another by conjugating with  $X$  gates. We likewise have  $X|T\rangle = e^{i\pi/8}|T^\dagger\rangle$ .

*g. CNOT and CS* Commuting CS through CNOT simply flips the phase of CS to  $SI \cdot CS^\dagger$ , which is the same as commuting CS through an  $X$  gate on the target qubits. Hence, we have the following identity for CNOT acting on the CS state:

$$\begin{array}{c} \text{CS state} \\ \boxed{|+\rangle} \\ \bullet \\ \text{---} \\ \bullet \end{array} \text{---} \begin{array}{c} \bullet \\ \text{---} \\ \oplus \\ \text{---} \\ \bullet \end{array} \text{---} = \begin{array}{c} \bullet \\ \text{---} \\ \bullet \\ \text{---} \\ \oplus \end{array} \text{---} \boxed{S} \text{---} = \begin{array}{c} \text{CS state} \\ \boxed{|+\rangle} \\ \bullet \\ \text{---} \\ \bullet \end{array} \text{---} \begin{array}{c} \bullet \\ \text{---} \\ \oplus \\ \text{---} \\ \bullet \end{array} \text{---} \boxed{X} \text{---}$$

## Appendix B: Faulty $|T\rangle$ states

When talking about the fault tolerance of the distillation and synthillation schemes considered in this work we start by adopting a common assumption that  $|T\rangle$  states are the faulty elements in our circuits and other Clifford components (mainly CNOTs) are implemented ideally. In this regard we have used  $T$  gates and  $|T\rangle$  states interchangeably throughout this work since we can implement  $T$  with  $|T\rangle$  by means of an adaptive gadget.



When  $T$  gates are implemented through such a gadget the associated noise channel typically takes the form

$$p_I\rho + p_S S\rho S^\dagger + p_{S^\dagger} S^\dagger\rho S + p_Z Z\rho Z^\dagger$$

Exactly how the channel error rates  $p_S$ ,  $p_Z$  and  $p_{S^\dagger}$  relate to the Pauli error rates of the original faulty  $T$  gate or state will depend on the specific gadget, but for many known gadgets the implemented  $T$  gates have noise of this form.

In our schemes however, not all  $|T\rangle$  states are used for injection; the data qubits are prepared in  $|T\rangle$ , meaning that  $X$ ,  $Y$  and  $Z$  errors are introduced to the data

qubits without first being mediated by a gadget. This does not impact the fault tolerance of these schemes because  $X|T\rangle = e^{i\pi/8}|T^\dagger\rangle = e^{i\pi/8}S^\dagger|T\rangle$  and similarly  $Y|T\rangle = e^{-i\pi/8}Z|T^\dagger\rangle = e^{-i\pi/8}S|T\rangle$ . Therefore, the noise model of the  $T$  states is the same as from the  $T$  gates of our scheme, though there may be differences in the specific error rates from the gadget used. For  $|T\rangle$  with Pauli error rates  $p'_X$ ,  $p'_Y$  and  $p'_Z$  we have  $p_{S^\dagger} = p'_X$ ,  $p_S = p'_Y$  and  $p_Z = p'_Z$ .

As a final note:  $S\rho S^\dagger + S^\dagger\rho S = \rho + Z\rho Z^\dagger$ , meaning that many sources of  $S$  and  $S^\dagger$  noise can be collected and re-expressed as  $Z$  noise when  $p_S = p_{S^\dagger}$ .

- 
- [1] L. Postler, S. Heußen, I. Pogorelov, M. Rispler, T. Feldker, M. Meth, C. D. Marciniak, R. Stricker, M. Ringbauer, R. Blatt, P. Schindler, M. Müller, and T. Monz, Demonstration of fault-tolerant universal quantum gate operations, *Nature* **605**, 675 (2022).
- [2] D. Bluvstein, S. J. Evered, A. A. Geim, S. H. Li, H. Zhou, T. Manovitz, S. Ebadi, M. Cain, M. Kalinowski, D. Hangleiter, J. P. Bonilla Ataides, N. Maskara, I. Cong, X. Gao, P. Sales Rodriguez, T. Karolyshyn, G. Semeghini, M. J. Gullans, M. Greiner, V. Vuletić, and M. D. Lukin, Logical quantum processor based on reconfigurable atom arrays, *Nature* **626**, 58 (2024).
- [3] C. Ryan-Anderson, N. C. Brown, C. H. Baldwin, J. M. Dreiling, C. Foltz, J. P. Gaebler, T. M. Gatterman, N. Hewitt, C. Holliman, C. V. Horst, J. Johansen, D. Lucchetti, T. Mengle, M. Matheny, Y. Matsuoka, K. Mayer, M. Mills, S. A. Moses, B. Neyenhuis, J. Pino, P. Siegfried, R. P. Stutz, J. Walker, and D. Hayes, High-fidelity teleportation of a logical qubit using transversal gates and lattice surgery, *Science* **385**, 1327 (2024).
- [4] R. Acharya, D. A. Abanin, L. Aghababaie-Beni, I. Aleiner, T. I. Andersen, M. Ansmann, F. Arute, K. Arya, A. Asfaw, N. Astrakhantsev, J. Atalaya, R. Babbush, D. Bacon, B. Ballard, J. C. Bardin, J. Bausch, A. Bengtsson, A. Bilmes, S. Blackwell, S. Boixo, G. Bortoli, A. Bourassa, J. Bovaird, L. Brill, M. Broughton, D. A. Browne, B. Buchea, B. B. Buckley, D. A. Buell, T. Burger, B. Burkett, N. Bushnell, A. Cabrera, J. Campero, H.-S. Chang, Y. Chen, Z. Chen, B. Chiaro, D. Chik, C. Chou, J. Claes, A. Y. Cleland, J. Cogan, R. Collins, P. Conner, W. Courtney, A. L. Crook, B. Curtin, S. Das, A. Davies, L. De Lorenzo, D. M. Debroy, S. Demura, M. Devoret, A. Di Paolo, P. Donohoe, I. Drozdov, A. Dunsworth, C. Earle, T. Edlich, A. Eickbusch, A. M. Elbag, M. Elzouka, C. Erickson, L. Faoro, E. Farhi, V. S. Ferreira, L. F. Burgos, E. Forati, A. G. Fowler, B. Foxen, S. Ganjam, G. Garcia, R. Gasca, É. Genois, W. Giang, C. Gidney, D. Gilboa, R. Gosula, A. G. Dau, D. Graumann, A. Greene, J. A. Gross, S. Habegger, J. Hall, M. C. Hamilton, M. Hansen, M. P. Harrigan, S. D. Harrington, F. J. H. Heras, S. Heslin, P. Heu, O. Higgott, G. Hill, J. Hilton, G. Holland, S. Hong, H.-Y. Huang, A. Huff, W. J. Huggins, L. B. Ioffe, S. V. Isakov, J. Iveland, E. Jeffrey, Z. Jiang, C. Jones, S. Jordan, C. Joshi, P. Juhas, D. Kafri, H. Kang, A. H. Karamlou, K. Kechedzhi, J. Kelly, T. Khaira, T. Khattar, M. Khezri, S. Kim, P. V. Klimov, A. R. Klots, B. Kobrin, P. Kohli, A. N. Korotkov, F. Kostritsa, R. Kothari, B. Kozlovskii, J. M. Kreikebaum, V. D. Kurilovich, N. Lacroix, D. Landhuis, T. Lange-Dei, B. W. Langley, P. Laptev, K.-M. Lau, L. Le Guevel, J. Ledford, J. Lee, K. Lee, Y. D. Lensky, S. Leon, B. J. Lester, W. Y. Li, Y. Li, A. T. Lill, W. Liu, W. P. Livingston, A. Locharla, E. Lucero, D. Lundahl, A. Lunt, S. Madhuk, F. D. Malone, A. Maloney, S. Mandrà, J. Manyika, L. S. Martin, O. Martin, S. Martin, C. Maxfield, J. R. McClean, M. McEwen, S. Meeks, A. Megrant, X. Mi, K. C. Miao, A. Mieszala, R. Molavi, S. Molina, S. Montazeri, A. Morvan, R. Movassagh, W. Mruczkiewicz, O. Naaman, M. Neeley, C. Neill, A. Nersisyan, H. Neven, M. Newman, J. H. Ng, A. Nguyen, M. Nguyen, C.-H. Ni, M. Y. Niu, T. E. O'Brien, W. D. Oliver, A. Opremcak, K. Ottosson, A. Petukhov, A. Pizzuto, J. Platt, R. Potter, O. Pritchard, L. P. Pryadko, C. Quintana, G. Ramachandran, M. J. Reagor, J. Redding, D. M. Rhodes, G. Roberts, E. Rosenberg, E. Rosenfeld, P. Roushan, N. C. Rubin, N. Saei, D. Sank, K. Sankaragomathi, K. J. Satzinger, H. F. Schurkus, C. Schuster, A. W. Senior, M. J. Shearn, A. Shorter, N. Shutty, V. Shvarts, S. Singh, V. Sivak, J. Skrzynny, S. Small, V. Smelyanskiy, W. C. Smith, R. D. Somma, S. Springer, G. Sterling, D. Strain, J. Suchard, A. Szasz, A. Szein, D. Thor, A. Torres, M. M. Torunbalci, A. Vaishnav, J. Vargas, S. Vdovichev, G. Vidal, B. Villalonga, C. V. Heidweiller, S. Waltman, S. X. Wang, B. Ware, K. Weber, T. Weidel, T. White, K. Wong, B. W. K. Woo, C. Xing, Z. J. Yao, P. Yeh, B. Ying, J. Yoo, N. Yosri, G. Young, A. Zalcman, Y. Zhang, N. Zhu, N. Zobrist, G. Q. AI, and Collaborators, Quantum error correction below the surface code threshold, *Nature* [10.1038/s41586-024-08449-y](https://doi.org/10.1038/s41586-024-08449-y) (2024).
- [5] D. Litinski, Magic State Distillation: Not as Costly as You Think, *Quantum* **3**, 205 (2019).
- [6] C. Chamberland and K. Noh, Very low overhead fault-tolerant magic state preparation using redundant ancilla encoding and flag qubits, *npj Quantum Information* **6**, 91 (2020).
- [7] T. Itogawa, Y. Takada, Y. Hirano, and K. Fujii, *Even more efficient magic state distillation by zero-level distillation* (2024), [arXiv:2403.03991 \[quant-ph\]](https://arxiv.org/abs/2403.03991).
- [8] C. Gidney, N. Shutty, and C. Jones, *Magic state cultivation: growing t states as cheap as cnot gates* (2024),

- arXiv:2409.17595 [quant-ph].
- [9] C. Jones, Low-overhead constructions for the fault-tolerant Toffoli gate, *Phys. Rev. A* **87**, 022328 (2013).
- [10] M. Amy, D. Maslov, and M. Mosca, Polynomial-time t-depth optimization of clifford+t circuits via matroid partitioning, *IEEE Transactions on Computer-Aided Design of Integrated Circuits and Systems* **33**, 1476 (2014).
- [11] P. Selinger, Quantum circuits of  $T$ -depth one, *Phys. Rev. A* **87**, 042302 (2013).
- [12] S. Bravyi and J. Haah, Magic-state distillation with low overhead, *Phys. Rev. A* **86**, 052329 (2012).
- [13] E. T. Campbell and M. Howard, Unified framework for magic state distillation and multiqubit gate synthesis with reduced resource cost, *Phys. Rev. A* **95**, 022316 (2017).
- [14] C. Gidney and A. G. Fowler, Efficient magic state factories with a catalyzed  $CCZ$  transformation, *Quantum* **3**, 135 (2019).
- [15] P. S. Rodriguez, J. M. Robinson, P. N. Jepsen, Z. He, C. Duckering, C. Zhao, K.-H. Wu, J. Campo, K. Bagnall, M. Kwon, T. Karolyshyn, P. Weinberg, M. Cain, S. J. Evered, A. A. Geim, M. Kalinowski, S. H. Li, T. Manovitz, J. Amato-Grill, J. I. Basham, L. Bernstein, B. Braverman, A. Bylinskii, A. Choukri, R. DeAngelo, F. Fang, C. Fieweger, P. Frederick, D. Haines, M. Hamdan, J. Hammett, N. Hsu, M.-G. Hu, F. Huber, N. Jia, D. Kedar, M. Kornjača, F. Liu, J. Long, J. Lopatin, P. L. S. Lopes, X.-Z. Luo, T. Macrì, O. Marković, L. A. Martínez-Martínez, X. Meng, S. Ostermann, E. Ostroumov, D. Paquette, Z. Qiang, V. Shofman, A. Singh, M. Singh, N. Sinha, H. Thoreen, N. Wan, Y. Wang, D. Waxman-Lenz, T. Wong, J. Wurtz, A. Zhdanov, L. Zheng, M. Greiner, A. Keesling, N. Gemelke, V. Vuletić, T. Kitagawa, S.-T. Wang, D. Bluvstein, M. D. Lukin, A. Lukin, H. Zhou, and S. H. Cantú, Experimental demonstration of logical magic state distillation, arXiv 10.48550/arXiv.2412.15165 (2024).
- [16] H. Zhou, C. Zhao, M. Cain, D. Bluvstein, C. Duckering, H.-Y. Hu, S.-T. Wang, A. Kubica, and M. D. Lukin, Algorithmic fault tolerance for fast quantum computing, arXiv 10.48550/arXiv.2406.17653 (2024).
- [17] D. Litinski, A Game of Surface Codes: Large-Scale Quantum Computing with Lattice Surgery, *Quantum* **3**, 128 (2019).
- [18] E. Murphy and A. Kissinger, Global synthesis of cnot circuits with holes, *Electronic Proceedings in Theoretical Computer Science* **384**, 75–88 (2023).
- [19] M. A. Webster, A. O. Quintavalle, and S. D. Bartlett, Transversal diagonal logical operators for stabiliser codes, *New Journal of Physics* **25**, 103018 (2023).
- [20] S. Bravyi and A. Kitaev, Universal quantum computation with ideal Clifford gates and noisy ancillas, *Phys. Rev. A* **71**, 022316 (2005).
- [21] A. G. Fowler and C. Gidney, Low overhead quantum computation using lattice surgery, arXiv (2019).
- [22] A. G. Fowler, M. Mariantoni, J. M. Martinis, and A. N. Cleland, Surface codes: Towards practical large-scale quantum computation, *Physical Review A* **86**, 10.1103/physreva.86.032324 (2012).
- [23] N. Fazio, R. Harper, and S. Bartlett, Logical noise bias in magic state injection (2024), arXiv:2401.10982 [quant-ph].
- [24] Z. Cai, A. Siegel, and S. Benjamin, Looped pipelines enabling effective 3D qubit lattices in a strictly 2D device, *PRX Quantum* **4**, 20345 (2023).